Ground-state magnetic resonance of $DyPO_4$ in the far infrared

G. A. Prinz, J. F. L. Lewis*, and R. J. Wagner
Naval Research Laboratory, Washington, D. C. 20375
(Received 28 May 1974)

Magnetic resonance has been observed in the Ising system $DyPO_4$ utilizing a far-infrared laser magnetic-resonance spectrometer, in applied fields $\vec{H} \| \vec{C}$ sufficient to saturate the spin system. The resonance spectra obtained at 220.23 μm (45.407 cm^{-1}) and 171.67 μm (58.25 cm^{-1}) at 4.2 °K were composed of three superimposed hyperfine patterns. Two of them were six-line patterns, one from $^{161}Dy^{3+}$ ($I = 5/2$) and one from $^{163}Dy^{3+}$ ($I = 5/2$). In addition there was a central line due to even isotopes ($I = 0$). All six lines of $^{163}Dy^{3+}$ were resolved, yielding a value for the spin-Hamiltonian parameter $^{163}(A/g_{\|}) = 37.2 \times 10^{-4}$ cm^{-1}, while for $^{161}Dy^{3+}$ we obtained $^{161}(A/g_{\|}) = 26.6 \times 10^{-4}$ cm^{-1} from the four components which could be resolved. From the two $I = 0$ resonances at 53 338 and 67 579 Oe, we obtain $g_{\|} = 19.32$. The effects of a large nonuniform demagnetizing field on the line shape have been observed and analyzed in detail.

I. INTRODUCTION

$DyPO_4$ is one member of a family of isomorphic rare-earth (RE) compounds including the RE orthovanadates, -arsenates, and -phosphates which possess the zircon crystal structure shown in Fig. 1.[1] This structure has the space symmetry of D_{4h}^{19} with the RE ions occupying sites of D_{2d} symmetry. While many of these compounds exhibit spontaneous crystalline distortions at low temperatures, $DyPO_4$ does not. It does, however, order antiferromagnetically at 3.39 °K. The ordered state has been determined from several investigations to be Ising-like in a two-sublattice arrangement as shown in Fig. 1.[2-4] In addition, in the ordered state a large magnetoelectric effect has been observed.[3] Studies using optical spectroscopy showed[5] that the ground state was extremely anisotropic, exhibiting a $g_{\|} = 19.5 \pm 0.4$ and $g_{\perp} = 0.5 \pm 0.5$. This anisotropy is the source of the observed Ising behavior. This same work[5] reported the somewhat surprising result, however, that heat-capacity measurements indicated a value for the hyperfine interaction about $\frac{1}{3}$ that reported for Dy^{3+} in $Y(CH_3COO)_3 \cdot 4H_2O$ (yttrium acetate).

The large value of $g_{\|}$ reported for the ground state of $DyPO_4$ indicated that magnetic resonance could be observed in the far infrared using magnetic fields available from superconducting solenoids. Several things could be learned from such a study. First, the question of the anomalously small hyperfine interaction inferred from heat-capacity measurements could be resolved by a direct spectroscopic measurement. Second, resonance spectra at these energies would reveal the presence of any low-lying electronic states, a crucial element in understanding the Ising-like behavior of this material. In addition, the strength of the observed resonances, if purely magnetic dipole, could yield a determination of $g_{\perp}$ independent from that obtained by visible spectroscopy.

The appearance of far-infrared molecular-gas lasers made possible the extension of magnetic-resonance studies from the microwave region up into the far infrared. This possibility was quickly exploited in the investigation of concentrated magnetic insulators.[6-8] Previously, magnetic ions were generally studied as low-concentration impurities in diamagnetic hosts in order to avoid the line broadening caused by coupling between magnetic ions. When the high magnetic fields employed in moving a resonance into the infrared can effectively saturate the spin system, the resonance will sharpen even in highly concentrated magnetic materials. After our first reported observation of the ground-state magnetic resonance of $DyPO_4$,[8] improvement of the experimental facilities permitted the resonance to be obtained at two separate frequencies and with resolution sufficient to observe the hyperfine structure. A preliminary report of these results was presented at the 16th Annual Conference on Magnetism and Magnetic Materials.[9] In the present paper we report these results in detail.

We shall first discuss the experimental technique, then consider the results obtained for the splitting factor and the effective fields caused by ion-ion coupling and shape-dependent demagnetizing effects, and finally evaluate the observed hyperfine structure.

II. EXPERIMENTAL TECHNIQUE

The details of our experimental technique have been thoroughly reported elsewhere,[10] so only a brief description will be given here. The magnetic-resonance spectrometer system is shown schematically in Fig. 2. The radiation emitted by the molecular-gas laser is passed through a mono-

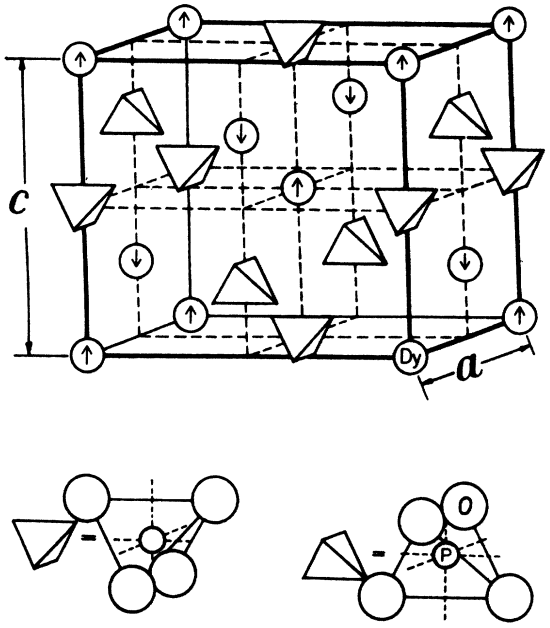

FIG. 1. Unit cell of $DyPO_4$: $a = 6.917$ Å, $c = 6.053$ Å. The arrows at the Dy^{3+}-ion sites indicate the moments in the antiferromagnetic state. The Dy^{3+} site symmetry is D_{2d}. The structure's space symmetry is D_{4h}^{19}.

chromator to select out one of the several frequencies which may be present. The radiation is then passed through a beam splitter which directs part of the light to a reference detector B. The remainder of the light is deflected to pass down the bore of a superconducting solenoid to another detector A. The two signals are amplified, and since the laser is run as a pulsed gas discharge, the pulsed signals are then passed to separate "boxcar" integrators (i.e., gated integrating amplifiers) which generate a dc level proportional to the integrated pulse. The two dc signals are then ratioed and the ratio A/B is displayed on one axis of an x-y recorder, the other axis being driven by a signal proportional to the strength of the solenoid's field. If a sample is placed in the solenoid bore one obtains directly a record of transmission versus applied magnetic field.

$DyPO_4$ was investigated using a crystal ($8.4 \times 2.3 \times 0.45$ mm), oriented as shown in Fig. 3, in which the applied magnetic field is parallel to the optic axis and the incident radiation propagates perpendicular to the optic axis. The radiation was polarized either σ ($\vec{E} \perp \vec{C}$) or π ($\vec{E} \parallel \vec{C}$) and the sample temperature was maintained at $4.2\,^{\circ}$K.

III. EXPERIMENTAL RESULTS

Figure 4 is an example of one of the observed resonances. There are two principal observations to make on the line shape: First, it has considerable structure, i.e., it is really a cluster of several resonance lines; second, it is decidedly asymmetric. The former is caused by the hyperfine interaction in the odd isotopes ^{161}Dy and ^{163}Dy. The latter is chiefly caused by the inhomogeneous demagnetizing field within the sample. We shall deal with the latter problem first since it alters the resonance field values which go into the analysis of the hyperfine interaction.

In this study, two separate laser frequencies were used. Magnetic resonance was obtained at 67 579-Oe applied field using the D_2O-vapor laser

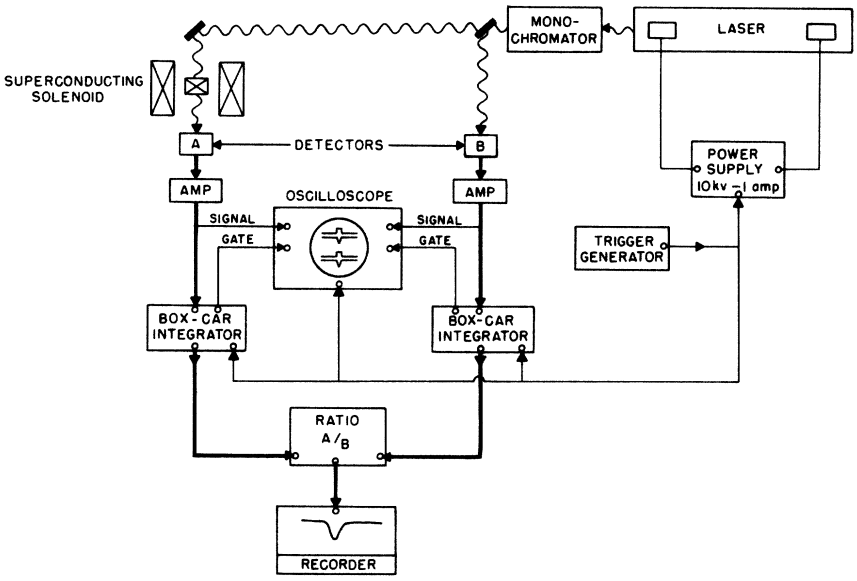

FIG. 2. Schematic diagram of magnetic-resonance spectrometer.

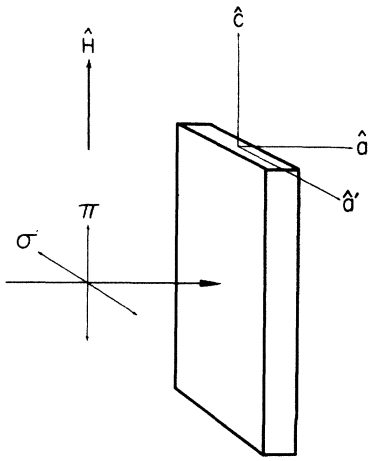

FIG. 3. Orientation of crystal sample with respect to the applied magnetic field H and the propagation of the incident radiation which is polarized π ($\vec{E} \parallel \vec{c}$) or σ ($\vec{E} \perp \vec{c}$). The edges of the sample are parallel to the unit cell directions $\hat{a}$, $\hat{a}'$, and $\hat{c}$.

frequency of 58.25 cm^{-1} (171.67 μm), and again at 53 338-Oe applied field using the H_2O-vapor laser frequency of 45.407 cm^{-1} (220.230 μm). Both were seen in π polarization only. From these two high-field points one obtains

$$g_{\parallel} \equiv \Delta\nu/\mu_B \Delta H = 19.32 \pm 0.01 \ ,$$

where $\mu_B = 0.46687 \times 10^{-4}$ cm^{-1}/Oe (Bohr magneton). This is in excellent agreement with the value $g_{\parallel} = 19.5 \pm 0.4$ obtained from optical spectroscopy,[5] and indicates that at least up to ≈ 60 cm^{-1} there is no coupling of the ground doublet to other low-lying states.

The observed resonances are obtained in a saturated paramagnet so that the effective resonance fields are not merely the applied magnetic fields. One must also consider the dipolar fields from the magnetic moments of the other Dy^{3+} ions in the sample and any additional effective fields due to other couplings between Dy^{3+} ions. The latter fields shall arbitrarily be grouped together under the heading "exchange."

Once the applied field is sufficiently high to saturate the paramagnetic system, any observed resonance frequency is then given by

$$\nu^{res} = g_{\parallel}\mu_B(H_{app}^{res} + H_{dip} + H_{ex}) , \qquad (1)$$

where H_{app}^{res} is the applied magnetic field at resonance, H_{dip} is the magnetic field at an ion site due to the dipolar moments of all the other Dy^{3+} ions in the sample when they are aligned with the applied field, and H_{ex} is any additional effective field due to other couplings between the aligned Dy^{3+} ions.

The dipolar field is calculated in the standard manner by first summing the contributions from individual dipoles within a sphere of radius R centered at an ion site and then enlarging R until the summation ceases to change. One then mathematically excises this sphere from the sample, and calculates the field due to the remaining surface polarizations. The inside surface is the Lorentz sphere and contributes $\frac{4}{3}\pi M_0$, where M_0 is the saturation magnetization. The contribution of the outside surface depends upon sample shape. It can be represented by a demagnetizing field DM_0, where D is a function which depends upon sample geometry and location within the sample. Thus we have

$$H_{dip} = H_{dip}^{\Sigma} + \tfrac{4}{3}\pi M_0 + DM_0 ,$$

where

$$H_{dip}^{\Sigma} = \sum_j \left(\frac{\vec{\mu}_j}{r_{ij}^3} - 3\frac{\vec{r}_{ij}(\vec{\mu}_j \cdot \vec{r}_{ij})}{r_{ij}^5} \right) .$$

Since all of the ions are Dy^{3+} in the ground state with their moments aligned along the tetragonal axis, we have for the magnetic moment per ion

$$|\vec{\mu}_j| = \mu_z = \tfrac{1}{2} g_{\parallel}\mu_B = 8.958 \times 10^{-20} \text{ erg/Oe (emu)} .$$

Carrying out the geometric summation to a 106-Å radius (a sphere containing 67×10^3 Dy^{3+} ions), one obtains a field

$$H_{dip}^{\Sigma} = 2125 \pm 5 \text{ Oe} .$$

The uncertainty represents the residual oscillations in the summation. This field is oppositely directed to H_{app} at the ion site.

The saturation magnetization M_0 is just the magnetic moment per cm^3 for all of the Dy^{3+}

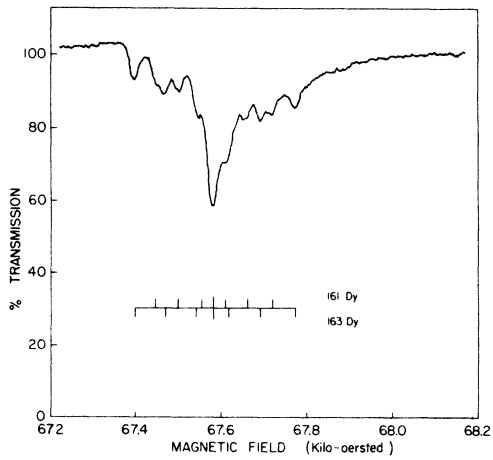

FIG. 4. Magnetic field dependence of the transmission of $DyPO_4$ at $\lambda = 171.67$ μm (58.25 cm^{-1}). The individual hyperfine components for $^{161}Dy^{3+}$ and $^{163}Dy^{3+}$ are indicated, as well as the central component for the even isotopes. The linewidth of an isolated component is 25 Oe.

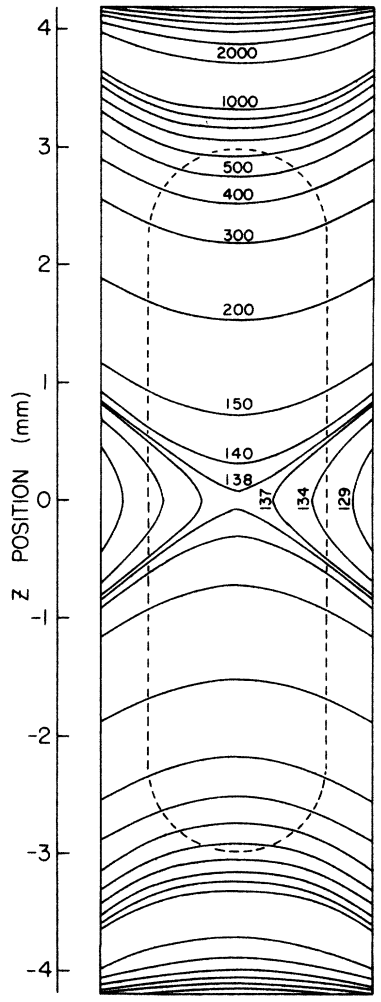

FIG. 5. Lines of constant demagnetizing field in the $x=0$ plane of our sample ($8.4\times2.3\times0.45$ mm). Field values are in units of Oe. The pattern is symmetric about $z=0$. The dashed lines indicate the aperture through which the transmission was measured.

aligned. Since there are four Dy^{3+} ions per unit cell, and the volume of a unit cell is 2.896×10^{-22} cm^3 ($6.917\times6.917\times6.053$ Å), we obtain $M_0=1237$ Oe. Hence the Lorentz field is $\frac{4}{3}\pi M_0=5181$ Oe. This field is directed parallel to H_{app} at the site.

The demagnetizing field in magnetized nonellipsoidal bodies has been considered by Joseph and Schlömann (JS).[11] In that paper they have assumed no g-factor anisotropy and have developed an expression for the demagnetizing field in the form of a converging series expansion in powers of M_0/H, the magnetization over the applied field. The Ising-like anisotropy of $DyPO_4$ makes it a very good approximation to assume that under the conditions of our experiments (in which the magnetization is saturated), the magnetization is perfectly uniform. This reduces the series expansion of JS to only the leading term. This remaining term yields a unidirectional but inhomogeneous demagnetizing field. The demagnetizing field becomes homogeneous only when a uniformly magnetized sample is ellipsoidal. For the form of the explicit expression applicable to our sample shape, rectangular prisms, we shall employ a rectangular coordinate system whose origin coincides with the center of the sample illustrated in Fig. 3, and whose coordinate axes are oriented $\vec{x}\parallel\hat{a}$, $\vec{y}\parallel\hat{a}'$, and $\vec{z}\parallel\hat{c}$. The end points of the sample in these three directions are given by $x=\pm A$, $y=\pm B$, and $z=\pm C$. For our sample $A:B:C\approx1:5:20$, with the saturation magnetization directed along z. From JS we then have the variation of the demagnetization field in the $y-z$ plane ($x=0$) given by

$$H_z\equiv DM_0=2M_0[\tan^{-1}g(y,z)+\tan^{-1}g(-y,z)+\tan^{-1}g(y,-z)+\tan^{-1}g(-y,-z)],$$

where

$$g(y,z)=\frac{A(B-y)}{(C-z)[A^2+(B-y)^2+(C-z)^2]^{1/2}}.$$

The variation along x is small, and has therefore been ignored. This distribution of the field in the sample is illustrated in Fig. 5, where lines of constant H have been drawn in the (y,z) plane with $x=0$. Our sample was mounted on a mask whose aperture is indicated by the dashed line in Fig. 5. Transmission therefore occurred only through this aperture, and we assume there was uniform intensity of the laser beam across it.

The spatial variation of the demagnetization field can significantly alter the observed shape of the resonance absorption line, since it will depend upon the intensity of radiation passing through each region of the crystal. These effects can be calculated by blocking the crystal into segments of approximately constant H to give the relative number of ions in each unit interval of demagnetizing field (Fig. 6). The transmission from each field interval is then summed, weighted by the number of ions in that interval. The resulting line will be asymmetrically broadened by the distribution shown in Fig. 6. If the single-ion line is much narrower than the width of the distribution at half-maximum (i.e., $\ll10$ Oe), the resulting line shape will be just that in Fig. 6, with the resonance-line peak shifted by 138 Oe. If the single-ion line is broad compared to the distribution, the result will be a broadened version of Fig. 6 with the maximum shifted to even higher fields. We shall see in Sec. IV that for the width derived from the best fit to the observed spectral profile the peak is shifted by an additional 21 Oe. This gives a total demagnetization field shift to the resonance-line peak of 159 Oe. This field is directed oppositely to H_{app}.

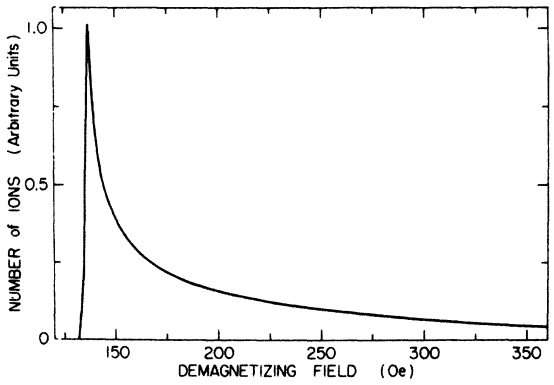

FIG. 6. Relative number of ions in a unit field interval as a function of demagnetizing field for the aperature shown in Fig. 5.

If we define a positive field as one in the same direction as the moments of the aligned ions, the summation of these contributions to the total dipolar field is

$$H_{dip} = -2125 + 5181 - 159 = 2897 \text{ Oe}.$$

We are now in a position to go back to Eq. (1) in order to estimate the nondipolar contributions to the internal field, H_{ex}. Choosing one of the particular resonances,

$$\nu^{res} = 45.407 = g_{\parallel}\mu_B(53\,338 + 2897 + H_{ex}).$$

Solving, we obtain

$$\nu_{ex} = g_{\parallel}\mu_B H_{ex} = -5.27 \text{ cm}^{-1},$$

the negative sign indicating an antiferromagnetic exchange field.

This nondipolar or "exchange" field energy can be divided into two contributions,

$$\nu_{ex} = \nu_{ex}^{nn} + \nu_{ex}^{\Sigma}, \tag{2}$$

where ν_{ex}^{nn} is due to the four aligned near neighbors (nn) and ν_{ex}^{Σ} is due to summing over the remaining Dy^{3+} ions. Optical spectroscopy in zero applied field yielded a measure of the near-neighbor dipolar-plus-nondipolar fields. It showed that[5]

$$\nu_0^{nn} = \nu_{dip}^{nn} + \nu_{ex}^{nn} = -7.35 \pm 0.20 \text{ cm}^{-1}.$$

Since ν_{dip}^{nn}, the nn dipolar energy, can be calculated to be

$$\nu_{dip}^{nn} = -3.07 \text{ cm}^{-1},$$

we have $\nu_{ex}^{nn} = -4.28 \text{ cm}^{-1}$. From Eq. (2) we obtain

$$\nu_{ex}^{\Sigma} = \nu_{ex} - \nu_{ex}^{nn} = -1.0 \pm 0.2 \text{ cm}^{-1}.$$

This result compares very well with that obtained from the optical spectra, where from measurements of line shifts below the antiferromagnetic ordering temperature and line shifts at the metamagnetic transition, it was concluded that[5]

$$\nu_{ex}^{\Sigma} = -1.0 \pm 0.5 \text{ cm}^{-1}.$$

IV. HYPERFINE INTERACTIONS

The remaining resonance feature seen in Fig. 4 is a cluster of absorption resonances arising from the hyperfine interaction in Dy^{3+}. To interpret this structure we note that for an odd-electron ion in D_{2d} site symmetry having an isolated Kramers-doublet ground state such as we have, the energy can be represented by the spin Hamiltonian

$$\mathcal{H} = \mu_B[g_{\parallel}S_z H_z + g_{\perp}(S_x H_x + S_y H_y)] + AS_z I_z + B(S_x I_x + S_y I_y) + P[I_z^2 - \tfrac{1}{3}I(I+1)].$$

The first term represents the Zeeman interaction, and since the applied field as well as the additional effective internal fields are along z, $H_x = H_y = 0$. The second and third terms represent the hyperfine coupling between the electron and the nucleus, and the fourth term is the quadrupole term.

The specific composition of the hyperfine constant can be written as[12]

$$A_i = \frac{2g_i\mu_N\mu_B\mu_I}{I}\langle r^{-3}\rangle\frac{\langle J \| N \| J\rangle}{\langle J \| \Lambda \| J\rangle}, \quad i = x, y, z$$

where μ_N is the nuclear magneton, μ_I is the nuclear magnetic moment, and $\langle r^{-3}\rangle$ is a radial integral of the $4f$ electron, r being the radius of the electron distribution measured from the nucleus. In this expression the Wigner-Eckert theorem has been used to replace the crystal-field dependence of the hyperfine operator $N = \sum[\vec{l} - \vec{s} + 3\vec{r}(\vec{r}\cdot\vec{s})/r^2]$ by the crystal-field dependence of the angular momentum operator $\Lambda = \vec{L} + 2\vec{S} = g_J\vec{J}$, since the two will differ by a constant dependent only on the J of the manifold. This constant is the ratio of the reduced matrix elements, which have been evaluated[13] for Dy^{3+}, and the crystal field dependence is in the g factor. Since $\langle r^{-3}\rangle$ for f electrons does not depend strongly upon the particular crystalline environment, to a good approximation the effect of local environment on the hyperfine constant is thus reflected only in the value of g_i. Hence A_i/g_i is constant for a given ion in different hosts. Furthermore, if $A_z \equiv A$, $g_z \equiv g_{\parallel}$, $A_x = A_y \equiv B$, and $g_x = g_y \equiv g_{\perp}$, as in $DyPO_4$, we may also conclude $A/g_{\parallel} = B/g_{\perp}$.

Previous work[14] on Dy^{3+} indicates this to be a very good approximation due to the $\approx 3300\text{-cm}^{-1}$ separation of the next highest free-ion level. Optical spectroscopy[5] indicated $g_{\perp} = 0.5 \pm 0.5$, and since $g_{\parallel} = 19.3$, we would conclude $B \approx 0.026A$. We shall therefore ignore the second hyperfine term.

The final term represents the nuclear quadrupole coupling to the crystalline electric field gradient. Since we are looking at transitions in which only the electron state changes ($\Delta S_z = \pm 1$ but $\Delta I_z = 0$), the

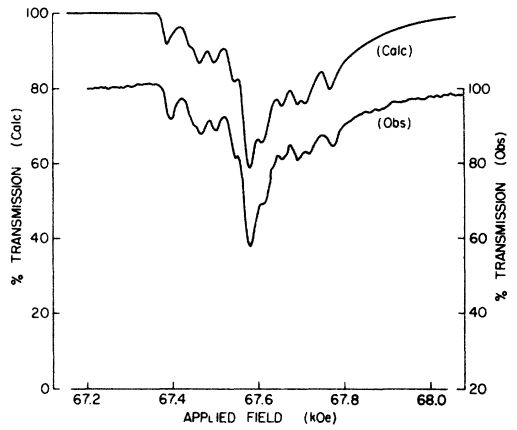

FIG. 7. Comparison of the observed resonance line profile with the best calculated fit. The broadening mechanism is the inhomogeneous demagnetization field illustrated in Fig. 5.

quadrupolar shift is the same in both the initial and final states of the transition, and thus is not observed. So we have the simple approximate spin Hamiltonian

$$\mathcal{H} = g_{\parallel}\mu_B S_z H_z + A S_z I_z . \tag{3}$$

There are actually three superimposed spectra: one six-line pattern arising from $^{161}Dy^{3+}$ ($I=\frac{5}{2}$), one six-line pattern from $^{163}Dy^{3+}$ ($I=\frac{5}{2}$), and the central line due to all of the even-mass isotopes which exhibit no hyperfine interaction. Isotopic abundances are $^{161}Dy : {}^{163}Dy : {}^{even}Dy = 18.7 : 24.9 : 56.4\%$. The basis for the six-line hyperfine patterns can be seen immediately if we rewrite Eq. (3) as

$$\mathcal{H} = g_{\parallel}\mu_B S_z [H_z + (A/g_{\parallel}\mu_B) I_z] .$$

Since I_z assumes the six values $+\frac{5}{2}, \ldots, -\frac{5}{2}$, we may regard the hyperfine interaction as merely adding an effective magnetic field which is quantized such that the resonances are spaced in six equal increments symmetrically about $I_z = 0$, with a spacing $\Delta H_z = A/g_{\parallel}\mu_B$. To obtain the hyperfine splitting from the observed spectra we constructed the thirteen-component pattern, with the relative strengths scaled to reflect the natural isotopic abundances, and then numerically integrated the spectrum over the demagnetization field distribution as discussed in Sec. III. The best fit of calculated to observed line shape was obtained using Gaussian lines of width 16 Oe, cross section at center $\sigma_0 = 1.34 \times 10^{-19}$ cm^2, and hyperfine field spacings of $\Delta H_z^{161} = 57 \pm 1$ Oe and $\Delta H_z^{163} = 80 \pm 1$ Oe. This calculated spectrum is shown with the observed spectrum in Fig. 7. To illustrate the dramatic effect of the inhomogeneous demagnetization field, the calculated spectrum is shown in Fig. 8 compared with the case of a uniform demagnetization field. Using $g_{\parallel} = 19.3$ and $\mu_B = 0.467 \times 10^{-4}$ cm^{-1}/Oe we obtain

$$A^{161} = 5.13 \times 10^{-2} \text{ cm}^{-1}, \quad A^{163} = 7.21 \times 10^{-2} \text{ cm}^{-1} .$$

It is of interest at this point to compare this result with earlier work on Dy^{3+}. From the previous discussion of the hyperfine constant we saw that A_i/g_i should be approximately constant for the ground state of a given ion, independent of the crystalline environment. In Table I our values for this ratio in $DyPO_4$ are compared with those for other Dy^{3+} compounds, and the agreement among the different compounds is excellent. We must therefore conclude that the anomalously low value for $A/g_{\parallel}$ in $DyPO_4$ which was predicted by others[5] on the basis of specific-heat measurements must be rejected.

The use of such large resonance fields might raise the question of the contribution of nuclear Zeeman splitting. The larger nuclear moment is reported for ^{163}Dy ($\mu_I = +0.64\mu_N$).[15] If we assume a field of 80 kOe, this would cause a shift in the ^{163}Dy hyperfine lines of

$$E = 2(0.64)(0.25 \times 10^{-7} \text{ cm}^{-1}/\text{Oe})(8 \times 10^4 \text{ Oe})$$
$$= 2 \times 10^{-3} \text{ cm}^{-1},$$

where $\mu_N = 0.25 \times 10^{-7}$ cm^{-1}/Oe. In terms of applied field this is ≈ 2 Oe, which is the order of the uncertainty in our data.

The unbroadened line shapes which we infer from our fitting procedure can be used to obtain an estimate of the oscillator strength. A Gaussian line of width at half-maximum of 16 Oe and $\sigma_0 = 1.34 \times 10^{-19}$ cm^2 yields an integrated cross section of $\int \sigma(\nu)\, d\nu = 6.12 \times 10^{-11}$ cm^2/sec. The index of refraction was

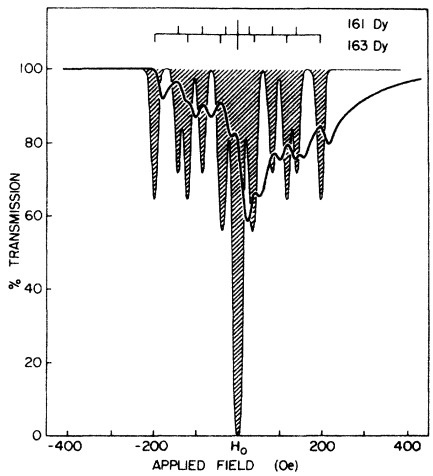

FIG. 8. Asymmetric profile (heavy outline) represents our best fit to the observed resonance, as shown in Fig. 7. The symmetric profile (crosshatched) is the unbroadened spectra one would observe for the same resonance in a homogeneous demagnetizing field.

TABLE I. Spin-Hamiltonian hyperfine constants. (All entries are in units of 10^{-1} cm^{-1}).

	Double nitrate[a]		Acetate[a]	Phosphate
	$A/g_{\parallel}$	$B/g_{\perp}$	A_x/g_x	$A/g_{\parallel}$
$^{161}Dy^{3+}$	27.13	27.6	27.9	26.6
$^{163}Dy^{3+}$	37.9	38.3	39.5	37.2

[a]Reference 12.

determined from the spacings of the channel spectrum obtained on a 170-μm-thick sample. The results are shown in Fig. 9 for the spectral region 90 to 160 cm^{-1}. The index falls rapidly as one moves to energies below the restrahlen region. Below 100 cm^{-1} the index apparently levels off to $n \approx 3$, the value we shall use. Thus the experimental determination of the oscillator strength is given by

$$f_{expt} = \left[\int \sigma(\nu)\, d\nu\right] \frac{mc}{\pi e^2} \frac{1}{n} = (6.12\times 10^{11})(37.68)(\tfrac{1}{3}) = (0.78 \pm 0.16)\times 10^{-9}.$$

In order to calculate the transition probability, we note that the lowest free-ion state of Dy^{3+} is $^6H_{15/2}$, and in a site of symmetry D_{2d} one obtains states containing m_J components which differ by $\Delta m_J = \pm 4$. The ground state $g_{\parallel} = 19.32$ which we observed is so large that the state is necessarily nearly pure $m_J = \pm\frac{15}{2}$. (Pure $m_J = \frac{15}{2}$ would yield $g_{\parallel} = 19.68$.) We can therefore conclude that the composition of the Kramers doublet is of the form $|\varphi \pm\rangle = a|\pm\tfrac{15}{2}\rangle + b|\pm\tfrac{7}{2}\rangle + c|\mp\tfrac{1}{2}\rangle + d|\mp\tfrac{9}{2}\rangle$. The only π transitions allowed within this doublet are magnetic dipole (MD), $\Delta m_J = \pm 1$.

Since the transition is magnetic dipole ($\Delta m_J = \pm 1$), the theoretical oscillator strength is

$$f_{MD} = (4.028\times 10^{-11}\ \text{cm})[\tilde{\nu}_{laser}\ (cm^{-1})] \times n\,|\langle\psi|L_x + 2S_x|\psi'\rangle|^2.$$

Our laser frequency is 58.25 cm^{-1} and $n \approx 3$, giving

$$f_{MD} = 7.04\times 10^{-9}\,|\langle\psi|L_x + 2S_x|\psi'\rangle|^2.$$

Equating this with the experimental strength, we find that

$$\langle\psi|L_x + 2S_x|\psi'\rangle \equiv \langle\psi|g_J J_x|\psi'\rangle = 0.33,$$

and thus

$$g_{\perp} \equiv 2\langle\psi|g_J J_x|\psi'\rangle = 0.7 \pm 0.1.$$

This compares well with the $g_{\perp} = 0.5 \pm 0.5$ (Ref. 5) obtained from optical-spectroscopy Zeeman-splitting measurements.

V. DISCUSSION

The good general agreement between the observed line profile and the one calculated from the known variation in the demagnetizing field indicates that demagnetization effects cannot be ignored when dealing with finely detailed resonance spectra. The precision to which agreement could be obtained in the fitting procedure was limited by the signal-to-noise in the laser output, the nonuniformities in the rate in which the applied magnetic field was swept, and by the assumption of uniform illumination of the sample.

The obvious way to eliminate such effects is to form spherical samples, but because of the strong absorption in concentrated materials, a sufficiently short absorption length would require an impractically small aperture. A more practical approach is to obtain thin samples of large surface area, and mask off all but the center section. Although large thin samples were not available to us, an additional resonance spectrum was obtained at $\lambda = 220.23$ μm (45.407 cm^{-1}) on the present sample after masking the aperture down to ± 1.05 mm in the z direction. While this did cause a further deterioration in signal-to-noise, we observed both a distinct sharpening of the hyperfine structure, and a contraction of the high-field tail, exactly as expected on the basis of the demagnetizing field distribution.

We have not included any quantitative discussion of possible interference phenomena. Such effects arise whenever one passes plane parallel monochromatic radiation through samples which are plane parallel dielectric slabs. The use of laser sources for far-infrared magnetic resonance can make these effects particularly striking. They were first reported as being seen in the cyclotron-resonance spectra of InSb,[16] and have since been seen by others.[17,18] The only evidence of interference in our spectra can be seen in Fig. 4, where the transmission on the low-field side of the resonance rises slightly above the level seen far from the resonance. A detailed analysis of these optical

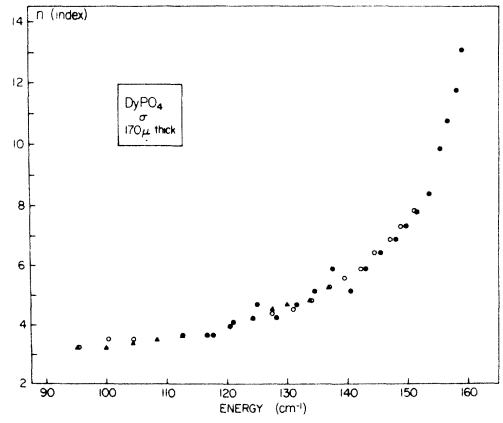

FIG. 9. Index of refraction of $DyPO_4$, obtained from the fringe spacings of channel spectra of a 170-μm-thick sample.

effects for our samples was unjustified because of the sample's poor optical quality. Microscopic investigation of the sample thickness indicated a step structure on the surfaces, causing thickness variations of 30 to 40 μm. A far-infrared index of refraction of ≈ 3.0 implies that these variations amount to $\approx \lambda/2$ at our laser wavelengths. Repeated attempts to cut, grind, or polish our samples resulted only in fracturing them. These very brittle flux-grown samples appear to be composed of many long thin crystals adhered together much like the individual boards in flooring. Since any observed interference effects in the resonance spectrum would be a weighted average over the whole sample, we have assumed they are sufficiently varied to have largely canceled.

VI. CONCLUSION

We have observed magnetic resonance in the concentrated paramagnetic $DyPO_4$ in fields high enough to saturate the spin system. The resonance frequencies, in the far infrared, were generated by a pulsed molecular-gas laser. Sufficient resolution was available to see the details of the hyperfine structure from the odd isotopes ^{161}Dy and ^{163}Dy. The hyperfine constants of the spin Hamiltonian thus obtained agree very well with the hyperfine interaction found in other Dy^{3+} compounds. The speculations which had been made by others concerning an anomalously low hyperfine interaction in $DyPO_4$ have therefore been found to be unsubstantiated. Values which we calculate from our data for magnetic near-neighbor interactions, and the ground-state g-factor components $g_{\parallel}$ and $g_{\perp}$, agree well with the results obtained from optical spectroscopy by others. Finally, a detailed analysis has shown that for materials composed of such high-moment ions, the effects of an inhomogeneous demagnetizing field upon the resonance line shape can be very important. In those cases where nonellipsoidal sample shapes are unavoidable, precise calculation of the inhomogeneous line broadening can be very successful at reproducing the observed resonance line profile.

---

*National Research Council–Naval Research Laboratories Research Associate.

[1]R. W. G. Wyckoff, *Crystal Structures*, 2nd ed. (Interscience, New York, 1965), Chap. VIII.
[2]J. C. Wright and H. W. Moos, Phys. Lett. A 29, 495 (1969).
[3]G. T. Rado, Phys. Rev. Lett. 23, 644 (1969).
[4]J. H. Colwell, B. W. Mangum, D. D. Thornton, J. C. Wright, and H. W. Moos, Phys. Rev. Lett. 23, 1245 (1969).
[5]J. C. Wright, H. W. Moos, J. H. Colwell, B. W. Mangum, and D. D. Thornton, Phys. Rev. B 3, 843 (1971).
[6]J. Boettcher, K. Dransfeld, and K. F. Renk, Phys. Lett. A 26, 146 (1968).
[7]J. P. Kotthaus and K. Dransfeld, Phys. Lett. A 30, 34 (1969).
[8]G. A. Prinz and R. J. Wagner, Phys. Lett. A 30, 520 (1969).
[9]G. A. Prinz and R. J. Wagner, J. Appl. Phys. 42, 1569 (1971).
[10]R. J. Wagner and G. A. Prinz, Appl. Opt. 10, 2060 (1971).
[11]R. I. Joseph and E. Schlömann, J. Appl. Phys. 36, 1579 (1965).
[12]J. G. Park, Proc. R. Soc. A 245, 118 (1958).
[13]R. J. Elliott and K. W. H. Stevens, Proc. R. Soc. A 218, 553 (1953).
[14]H. M. Crosswhite and G. H. Dieke, J. Chem. Phys. 35, 1535 (1961).
[15]Nucl. Data A 5, Nos. 5 and 6 (1969).
[16]B. D. McCombe, R. J. Wagner, and G. A. Prinz, Bull. Am. Phys. Soc. 15, 304 (1970).
[17]S. Roberts and I. S. Jacobs, AIP Conf. Proc. 10, 107 (1973).
[18]D. F. Nicoli and M. Tinkham, Phys. Rev. B 9, 3126 (1974).